Optimal operating conditions of an entangling two-transmon gate

2012 New J. Phys. 14 053035

(http://iopscience.iop.org/1367-2630/14/5/053035)

New Journal of Physics
The open-access journal for physics

Optimal operating conditions of an entangling two-transmon gate

Antonio D'Arrigo and Elisabetta Paladino
Dipartimento di Fisica e Astronomia, Università di Catania,
c/o Viale A Doria 6, Ed. 10, 95125 Catania, Italy
CNR—IMM—MATIS, c/o DFA Via Santa Sofia 64, 95123 Catania, Italy
E-mail: adarrigo@dmfci.unict.it and epaladino@dmfci.unict.it

New Journal of Physics **14** (2012) 053035 (11pp)
Received 31 January 2012
Published 25 May 2012
Online at http://www.njp.org/
doi:10.1088/1367-2630/14/5/053035

Abstract. We identify the optimal operating conditions of an entangling two-qubit gate realized by capacitive coupling of two superconducting charge qubits in a transmission line resonator (the so-called 'transmons'). We demonstrate that the sensitivity of the optimized gate to $1/f$ flux and critical current noise is suppressed to leading order. The procedure only requires a preliminary estimate of the $1/f$ noise amplitudes. No additional control or bias line beyond those used for the manipulation of individual qubits is needed. The proposed optimization is effective also in the presence of relaxation processes and of spontaneous emission through the resonator (Purcell effect).

Contents

1. Introduction

Superconducting circuits are a promising technology for the realization of quantum information on a solid state platform. Several types of qubits ([1] and references therein) have been developed realizing high-fidelity single-qubit operations [2, 3]. Rapid progress has also been made towards the realization of robust and scalable universal two-qubit gates [4–6]. The circuit quantum electrodynamics (cQED) [7] architecture was demonstrated to be particularly promising for scalable quantum information. In this scheme highly entangled two [8, 9] and three qubits [10] have been generated and simple quantum algorithms have been demonstrated [11, 12].

The coherence times of the present generation of devices ($\sim \mu$s) are about three orders of magnitude larger than the first implementations. A relevant step further toward this enhancement has been the elimination of linear sensitivity to low-frequency ($1/f$) noise by operating qubits at 'optimal' working points. After the first 'sweet spot' operation demonstrated in [3], a further boost of qubit performances has been achieved in a cQED design named 'transmon' [13], which is almost insensitive to the detrimental effect of $1/f$ charge noise [14] at the price of reduced anharmonicity. However, cQED architectures share with other implementations the presence of $1/f$ flux noise whose amplitude has a characteristic order of magnitude [15] and of $1/f$ critical current noise [13]. Together with relaxation processes due to quantum noise, dephasing due to $1/f$ flux and critical current noise still limits the time scales over which phase coherence and *entanglement* are preserved. In fact, further improvement of the coherence times at least of one order of magnitude would be required to reach the level for practical quantum error correction [16]. Recently, in a new cQED architecture employing a three-dimensional resonator the error correction threshold has been approached [17]. 'Optimization' is thus a key word of the present generation of superconducting nano-circuits. Clever circuit design and optimal tuning of multi-qubit architectures, supplemented with the use of improved materials, are two complementary strategies currently exploited to address this problem.

A major question that remains unsolved is establishing the best strategy to maintain for long enough a sufficient degree of entanglement. In this work, we address this issue considering a universal two-qubit gate realized by a fixed capacitive coupling of two transmons in a cQED architecture. The implementation of this scheme has recently been reported in [9], where a $\sqrt{\mathrm{i-SWAP}}$ operation (defined at the end of section 2) with individual single-shot non-destructive readout [18] and gate fidelity of 90%, partly limited by qubit decoherence, has been demonstrated. A similar system has been studied theoretically in [19, 20]. Here we identify the 'optimal' [21] operating conditions of a transmons $\sqrt{\mathrm{i-SWAP}}$ gate taking into account the multi-level nature of the nano-circuit. We find that an 'optimal coupling' exists where the leading order effects of $1/f$ flux and critical current noise are eliminated. The amount of preserved entanglement is quantified by the concurrence between the two transmons, $C(t)$, which we evaluate in analytic form. The efficiency of the 'optimal coupling' is demonstrated by the fact that, for typical $1/f$ noise spectra measured in superconducting nano-circuits, the concurrence is predicted to decay on a time scale [22] $T_2^{*\mathrm{SWAP}} \gtrsim 300\,\mu$s (in the absence of other decay mechanisms). In addition, $C(t)$ may attain values [23] guaranteeing violation of a Bell inequality until $\sim 80\,\mu$s and the gate fidelity is 99% up to $\sim 20\,\mu$s. Finally, we demonstrate that the optimization is effective also in the presence of relaxation processes due to flux quantum noise. Similarly to other cQED systems [24], the gate efficiency can be limited by spontaneous emission through the resonator. This limitation is likely to be overcome by suitable Purcell

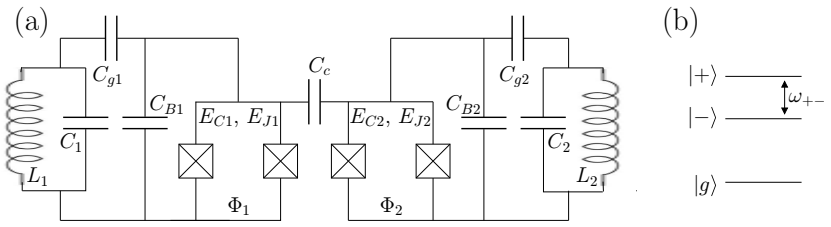

Figure 1. (a) Circuit diagram of the two transmon gate with capacitive coupling energy $E_{CC} = (2e)^2 C_T / C_{\Sigma 1} C_{\Sigma 2}$, where $1/C_T = 1/C_c + 1/C_{\Sigma 1} + 1/C_{\Sigma 2}$ and $C_{\Sigma\alpha} = C_{J\alpha} + C_{g\alpha} + C_{B\alpha}$. (b) Schematic level structure.

filters or protected designs [25]. The optimization proposed in the present paper can further improve the considerable performance of cQED two-qubit gates based on cavity-mediated interaction [10, 12] or on tunable effective interaction with microwave control [26]. Remarkably, here effective elimination of omnipresent $1/f$ noise sources is achieved even if one qubit does not operate at optimal bias and without additional controls or bias lines beyond those used for the manipulation of individual qubits, an important feature for scalability.

2. The universal two-transmon gate

We consider two transmons with a fixed capacitive coupling, each qubit being embedded in its superconducting resonator used for control and bit-wise readout [9, 18]. The interaction is effectively switched on/off by dynamically changing the qubits detuning using single-qubit control lines. For this reason, one of the qubits does not operate at its sweet spot. In figure 1(a), we report the circuit diagram of the considered system. Each transmon, denoted by the subscript $\alpha = 1, 2$, consists of a Cooper pair box (CPB) characterized by the charging energy $E_{C\alpha}$ and the Josephson energy $E_{J\alpha} = E^0_{J\alpha}\cos(\phi_\alpha)$, tunable via the magnetic flux threading the superconducting loop, $\phi_\alpha = \pi\,\Phi_\alpha/\Phi_0$ (Φ_0 is the flux quantum). In the circuit-QED scheme each CPB is embedded in a transmission line resonator whose relevant mode is modeled as an LC oscillator [13]. Thus the Hamiltonian of transmon α consists of the CPB Hamiltonian plus the dipole-like interaction with the LC oscillator [13]

$$\mathcal{H}_\alpha = E_{C\alpha}(\hat{q}_\alpha - q_{x,\alpha})^2 - E_{J\alpha}(\phi_\alpha)\cos\hat{\varphi}_\alpha + \omega_{r\alpha}\, a^\dagger_\alpha a_\alpha + 2\beta_\alpha e V_\alpha\, \hat{q}_\alpha\,(a_\alpha + a^\dagger_\alpha)\,, \qquad (1)$$

where the phase, $\hat{\varphi}_\alpha$, and charge, $\hat{q}_\alpha$, are conjugate variables, $[\hat{\varphi}_\alpha, \hat{q}_\alpha] = \mathrm{i}$. The resonator energy is $\omega_{r\alpha} = 1/\sqrt{L_\alpha C_\alpha}$ and $a^\dagger_\alpha$ (a_α) creates (annihilates) one photon in the transmission line ($\hbar = 1$). $V_\alpha = \sqrt{\omega_{r\alpha}/2C_\alpha}$ is the root-mean-square voltage of the oscillator and $\beta_\alpha = C_{g\alpha}/C_{\Sigma\alpha}$ is the ratio between the gate capacitance coupling the CPB to the local mode and the CPB total capacitance.

The transmon operates at $E_{C\alpha} \ll E^0_{J\alpha}$. Under these conditions, values of the phases φ_α close to zero are most favored. This motivates the neglect of the periodic boundary condition on the phases and the expansion of the cosine in equation (1). Within this approximation, the offset charge $q_{x,\alpha}$ can be eliminated via a gauge transformation [13]. Of course, the perturbative scheme cannot capture the non-vanishing charge dispersion of the transmon [27, 28]. In particular, the exponential decrease of the charge dispersion with $\sqrt{E^0_{J\alpha}/E_{C\alpha}}$ for $E^0_{J\alpha}/E_{C\alpha} \gg 1$ only results from the exact diagonalization of the CPB Hamiltonian in the phase basis [13]. It leads to exponential suppression of sensitivity to low-frequency ($1/f$) fluctuations of the offset

charge [14]. Here we rely on this well-established result and eliminate $q_{x,\alpha}$ from the outset. Expanding the cosine in equation (1) up to fourth order, the CPB Hamiltonian can be cast in the form of a weakly anharmonic oscillator (Duffin oscillator)

$$\mathcal{H}_\alpha^{\mathrm{D}} = \Omega_\alpha\, b_\alpha^\dagger b_\alpha - (E_{\mathrm{C}\alpha}/48)(b_\alpha + b_\alpha^\dagger)^4\,, \tag{2}$$

where the bosonic operators b_α, $b_\alpha^\dagger$ are related to the charge operator via $\hat{q}_\alpha = -\mathrm{i}(E_{\mathrm{J}\alpha}/2E_{\mathrm{C}\alpha})^{1/4}(b_\alpha - b_\alpha^\dagger)/\sqrt{2}$ and we put $\Omega_\alpha \equiv \Omega_\alpha(\phi_\alpha) = \sqrt{2E_{\mathrm{C}\alpha}E_{\mathrm{J}\alpha}(\phi_\alpha)}$. The two lowest eigenenergies of $\mathcal{H}_\alpha^{\mathrm{D}}$ identify the transmon-α qubit levels. Their splitting is $\tilde{\Omega}_\alpha = \Omega_\alpha - E_{\mathrm{C}\alpha}/4$ and it can be tuned by changing the magnetic flux Φ_α. The flux 'sweet-spot' is at $\phi_\alpha = 0$ [3, 13].

The capacitive coupling between the CPBs, $E_{\mathrm{CC}}(\hat{q}_1 - q_{x,1})(\hat{q}_2 - q_{x,2})$, adds to $\sum_\alpha \mathcal{H}_\alpha$, leading to the Hamiltonian

$$\mathcal{H} = \mathcal{H}_1^{\mathrm{D}} + \mathcal{H}_2^{\mathrm{D}} + \frac{\bar{E}_{\mathrm{CC}}}{2}(b_1 - b_1^\dagger)(b_2 - b_2^\dagger), \tag{3}$$

where $\bar{E}_{\mathrm{CC}} = E_{\mathrm{CC}}(E_{\mathrm{J}1}E_{\mathrm{J}2}/4E_{\mathrm{C}1}E_{\mathrm{C}2})^{1/4}$ is the effective coupling depending on the control parameters ϕ_α via the Josephson energies. Note that fluctuations of the magnetic fluxes affect the effective coupling between the qubits. Typical values [9] are $E_{\mathrm{C}\alpha} \sim 1\,\mathrm{GHz}$ and $E_{\mathrm{J}\alpha}^0 \sim$ 20–30 GHz, leading to $\bar{E}_{\mathrm{CC}} = 10^{-1}$–$10^{-2}\,\mathrm{GHz}$.

The coupled transmon eigenenergies and eigenstates are conveniently obtained by treating in perturbation theory with respect to $\sum_\alpha \Omega_\alpha\, b_\alpha^\dagger b_\alpha$ both the anharmonic terms and the capacitive interaction included in

$$V = \frac{\bar{E}_{\mathrm{CC}}}{2}(b_1 - b_1^\dagger)(b_2 - b_2^\dagger) - \sum_\alpha \frac{E_{\mathrm{C}\alpha}}{48}(b_\alpha + b_\alpha^\dagger)^4. \tag{4}$$

The level structure is schematically shown in figure 1(b). The splitting in the subspace where the SWAP operation takes place (in short 'SWAP splitting') reads $\omega_{+-} = \sqrt{(\tilde{\Omega}_1 - \tilde{\Omega}_2)^2 + \bar{E}_{\mathrm{CC}}^2}$ and the corresponding eigenstates spanning the 'SWAP subspace' are $|-\rangle = -\sin(\eta/2)|01\rangle + \cos(\eta/2)|10\rangle$ and $|+\rangle = \cos(\eta/2)|01\rangle + \sin(\eta/2)|10\rangle$, where $\tan\eta = \bar{E}_{\mathrm{CC}}/(\tilde{\Omega}_1 - \tilde{\Omega}_2)$ and $|a,b\rangle \equiv |a\rangle_1|b\rangle_2$ are eigenstates of $\sum_\alpha \Omega_\alpha\, b_\alpha^\dagger b_\alpha$ ($a,\, b \in \{0,1\}$). The interaction is effectively switched on by tuning the single-qubit energy spacing to mutual resonance. The resonance condition is realized by tuning the flux bias until $\tilde{\Omega}_1 = \tilde{\Omega}_2$, displacing one qubit from the sweet spot at $\phi_\alpha = 0$. In the following we suppose that $\phi_1 = 0$ and $\phi_2 \neq 0$. Under resonance conditions the $\sqrt{\mathrm{i-SWAP}}$ operation $|01\rangle \to |\psi_{\mathrm{e}}\rangle = [|01\rangle - \mathrm{i}|10\rangle]/\sqrt{2}$ is realized by free evolution for a time $t_{\mathrm{E}} = \pi/2\omega_{+-}$ starting from a factorized initial state in the 'SWAP subspace'.

3. Optimal operating conditions: reduction of $1/f$ noise effects

Since the two qubits do not operate at the same working point, the dominant source of dephasing is different for the two transmons. In particular, first-order fluctuations of the transmon splittings are due to $1/f$ critical current noise for transmon 1 and to $1/f$ flux noise for transmon 2 [13]. These fluctuations can be treated in the adiabatic and longitudinal approximation [29] by replacing $E_{\mathrm{J}\alpha}$ with $E_{\mathrm{J}\alpha}(1 + x_\alpha(t))$. Here $x_\alpha(t)$ represent stochastic fluctuations of the dimensionless critical current $x_1(t) = \delta I_{\mathrm{c}1}(t) = \Delta I_{\mathrm{c}1}(t)/I_{\mathrm{c}1}$ and of the flux Φ_2, $x_2(t) = \tan(\phi_2)\,\delta\phi_2(t)$. The leading order effect of adiabatic noise is defocusing, expressed by the 'static path' or static noise approximation (SPA) [29, 30] describing the average of signals oscillating at randomly distributed effective frequencies (see the appendix for the validity

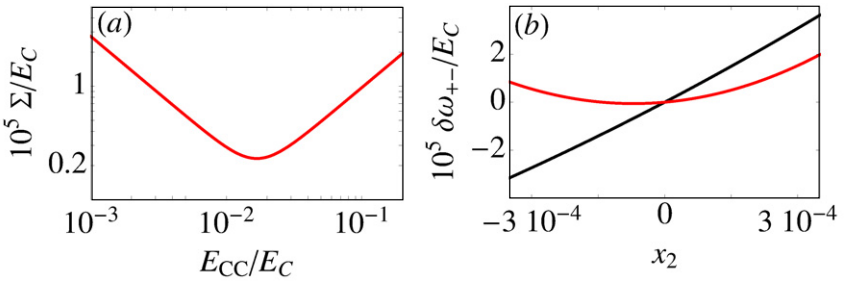

Figure 2. (a) SWAP-splitting variance equation (6) as a function of E_{CC}/E_C. The value of the minimum of Σ at the optimal point $E_{CC}^{opt} = 2E_C(\Sigma_{x_2}/\sqrt{2})^{1/2} = 1.68 \times 10^{-2} E_C$ is one order of magnitude smaller than at $E_{CC} = 10^{-1} E_C$. (b) Dispersion branch $\delta\omega_{+-}(x_2, x_1 = 0)/E_C$ for $|x_2| \leqslant 3\Sigma_{x_2}$. The black line is for a generic coupling $E_{CC} = 10^{-1} E_C$ and the red line is for the optimal coupling E_{CC}^{opt}. Parameters are $E_{C\alpha} = 1$ GHz, $E_{J\alpha}^0 = 30 E_{C\alpha}$ with $\phi_2 = 0.64$ and $\Sigma_{x_2} = 10^{-4}$.

regimes of the SPA in the present problem). It is obtained by replacing $x_\alpha(t)$ with statistically distributed values x_α. In the SPA the coherence between the states $|\pm\rangle$ is

$$\langle \rho_{+-}(t) \rangle \;=\; \rho_{+-}(0)\, \mathrm{e}^{-\mathrm{i}\omega_{+-}t}\, \langle \mathrm{e}^{-\mathrm{i}\delta\omega_{+-}t} \rangle, \tag{5}$$

where $\rho(t)$ is the two-qubit density matrix and $\langle \cdots \rangle$ indicates the average over the fluctuations x_α. Here we assume that they are uncorrelated random variables with Gaussian distribution, zero mean and standard deviations Σ_{x_α} proportional to the amplitude of the $1/f$ spectrum, $S_{x_\alpha}^{1/f}(\omega) = \pi \Sigma_{x_\alpha}^2 [\ln(\gamma_{M\alpha}/\gamma_{m\alpha})\, \omega]^{-1}$ ($\gamma_{m\alpha}$ and $\gamma_{M\alpha}$ are the low- and the high-frequency cut-offs of the $1/f$ region). As demonstrated in [21, 22], the optimal operating condition is obtained imposing a minimum of the variance of the stochastic SWAP splitting, $\Sigma^2 = \langle \omega_{+-}^2 \rangle - \langle \omega_{+-} \rangle^2$. This is simply understood considering the short-time expansion $|\langle \mathrm{e}^{-\mathrm{i}\delta\omega_{+-}t} \rangle| \approx \sqrt{1 - (\Sigma t)^2}$, implying defocusing suppression when Σ is minimal. Expanding ω_{+-} around the fixed working point we get

$$\Sigma^2 \approx \sum_\alpha \left(\frac{\partial \omega_{+-}}{\partial x_\alpha} \right)^2 \Sigma_{x_\alpha}^2 + \frac{1}{2} \sum_{\alpha,\beta} \left(\frac{\partial^2 \omega_{+-}}{\partial x_\alpha \partial x_\beta} \right)^2 \Sigma_{x_\alpha}^2 \Sigma_{x_\beta}^2, \tag{6}$$

where all derivatives are evaluated at $x_\alpha \equiv 0$. At resonance we find that $\partial\omega_{+-}/\partial x_\alpha = \bar{E}_{CC}/4$, $\partial^2\omega_{+-}/\partial x_\alpha^2 = -3\bar{E}_{CC}/16 + \Omega^2/(4\bar{E}_{CC})$, $\partial^2\omega_{+-}/\partial x_1 \partial x_2 = -\bar{E}_{CC}/16 - \Omega^2/(4\bar{E}_{CC})$, where we put $\Omega_\alpha \equiv \Omega$, $E_{C\alpha} \equiv E_C$. The variance equation (6) is non-monotonic in the coupling energy (figure 2(a)) and its minimum depends on the noise variances $\Sigma_{x_\alpha}^2$. For typical values of the amplitudes of $1/f$ flux and critical current noise[1] the dominant effect is due to flux noise, $\Sigma_{x_2} \gg \Sigma_{x_1}$, and the optimal coupling is found at $E_{CC}^{opt} \approx 2E_C(\Sigma_{x_2}/\sqrt{2})^{1/2}$. Note that, since $\bar{E}_{CC}$ depends on x_α (via $E_{J\alpha}$), the differential dispersion $\partial\omega_{+-}/\partial x_\alpha$ at $x_\alpha = 0$ is non-vanishing unless the coupling is switched off. The condition of minimal variance effectively identifies an 'optimal' dispersion leading to minimal defocusing, see figure 2(b).

In addition we observe that, since E_{CC}^{opt} depends on E_C but not on the Josephson energy, the optimized SWAP frequency, $\omega_{+-}^{opt} \approx \bar{E}_{CC}^{opt}$, can be engineered by appropriately fixing (within the experimental tolerances) the ratios $E_{J\alpha}^0/E_{C\alpha}$. This recipe can be conveniently applied even if an

[1] Flux noise is $S^{1/2}(1\,\mathrm{Hz}) = 10\mu\Phi_0/\sqrt{\mathrm{Hz}}$ [13, 15, 18] leading to $\Sigma_{x_2} \approx 1.65 \times 10^{-4}$. From the critical current noise in [13], we obtain $\Sigma_{x_1} \approx 10^{-6}$. We assumed $\log(\gamma_{M\alpha}/\gamma_{m\alpha}) = 6$.

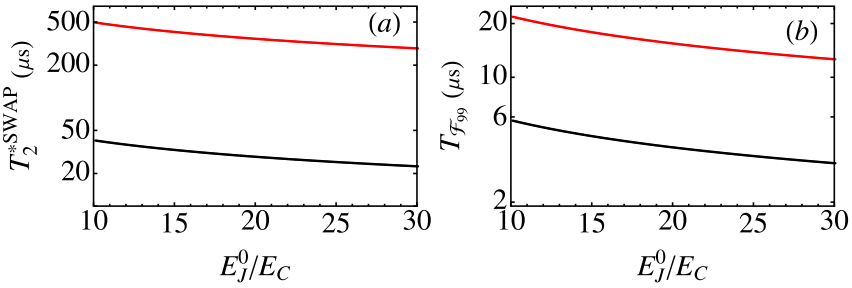

Figure 3. $T_2^{*\mathrm{SWAP}}$ (panel (a)) and $T_{\mathcal{F}_{99}}$ (panel (b)) as a function of $E_\mathrm{J}^0/E_\mathrm{C}$ for $E_{\mathrm{C}\alpha} = 1\,\mathrm{GHz}$. The variances $\Sigma_{x_1} = 5\times10^{-6}$, $\Sigma_{x_2} = 10^{-4}$ correspond to typical values of $1/f$ critical current and flux noise (see footnote 1) rescaled to the present setup. Black lines are obtained for $E_{\mathrm{CC}} = 10^{-1}E_\mathrm{C}$ and red lines correspond to $E_{\mathrm{CC}}^{\mathrm{opt}} = 1.68\times10^{-2}E_\mathrm{C}$.

independent estimate of the flux noise amplitude, Σ_{x_2}, for the specific setup is not available. In fact, the variance of the stochastic SWAP splitting, Σ^2, depends very smoothly on E_{CC} (figure 2(a)), allowing a practical estimate of $E_{\mathrm{CC}}^{\mathrm{opt}}$ based on the characteristic value of Σ_{x_2} observed in different flux and phase qubits. Alternatively, if different devices can be fabricated, one should select the sample with the ratio $E_{\mathrm{J}\alpha}^0/E_{\mathrm{C}\alpha}$ taking the right value for the given noise level of that particular device.

The effectiveness against defocusing of operating at the optimal coupling is revealed by the concurrence [32], which we evaluate in the SPA. We assume that the system is prepared in the state $|01\rangle$ and freely evolves. In the adiabatic approximation, populations are constant thus $C(t) \approx 2\,|\mathrm{Im}\langle\rho_{+-}(t)\rangle|$. Evaluating the integral (5) we obtain

$$C_{\mathrm{SPA}}(t) \approx \left| \mathrm{Im} \frac{\exp\left\{ -\frac{1}{2} \frac{\Sigma_{x2}^2 \left(\frac{\partial\omega_{+-}}{\partial x_2}\right)^2 t^2}{1+\mathrm{i}\Sigma_{x2}^2 (\frac{\partial^2\omega_{+-}}{\partial x_2^2})t} \right\}}{\sqrt{1+\mathrm{i}\Sigma_{x2}^2 (\frac{\partial^2\omega_{+-}}{\partial x_2^2})t}} \right| . \tag{7}$$

A measure of the entanglement preservation is the 'SWAP decay time' [22] defined by the condition $|C_{\mathrm{SPA}}(T_2^{*\mathrm{SWAP}})| = \mathrm{e}^{-1}$. At the optimal coupling, $T_2^{*\mathrm{SWAP}}$ is one order of magnitude larger than that for a generic coupling, assuming remarkable values up to $T_2^{*\mathrm{SWAP}} \sim 400\,\mu\mathrm{s}$ stable with increasing $E_\mathrm{J}^0/E_\mathrm{C}$ (figure 3(a)). In addition, a 99% fidelity to the Bell state $|\psi_{\mathrm{ent}}\rangle = [|01\rangle + |10\rangle]/\sqrt{2}$ is maintained up to $T_{\mathcal{F}_{99}} \approx 20\,\mu\mathrm{s}$, about *four* times longer than for a generic coupling (figure 3(b)). These results elucidate the capability of the proposed operating condition to drastically reduce the defocusing due to $1/f$ flux and critical current noise. On the other hand, energy relaxation processes are expected to limit the gate fidelity and the qubit relaxation times of the considered architecture [9]. In the following section, we discuss the robustness of the optimal coupling condition to relaxation processes.

4. Optimal operating conditions: robustness to relaxation processes

We now discuss the robustness of the above optimization against relaxation processes due to flux noise and to spontaneous emission through the resonator. Flux quantum noise is due to the

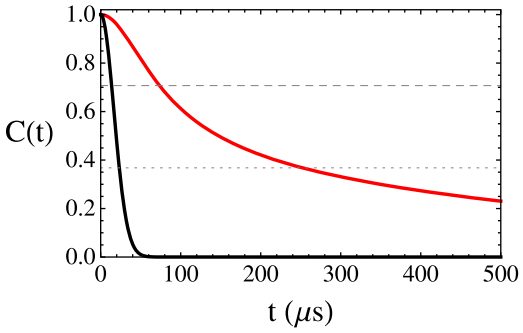

Figure 4. Envelope of the concurrence in the presence of $1/f$ flux and critical current noise (as in figure 3) and flux quantum noise on qubit 2 with spectrum $S_{x_2}(\omega) \simeq 10^{-9}\omega$. The black line is for $E_{\rm CC} = 10^{-1}E_{\rm C1}$; the red line is for $E_{\rm CC}^{\rm opt} = 1.68 \times 10^{-2}E_{\rm C1}$. The dashed gray line marks the value $C = 1/\sqrt{2}$ and the dotted line $C(T_2^{\rm SWAP}) = {\rm e}^{-1}$.

external magnetic flux bias through a mutual inductance M [13] and it enters the Josephson energies in $\mathcal{H}_{\rm D}$ and in $\bar{E}_{\rm CC}$. It is included by adding to $\mathcal{H}$, equation (3), the terms

$$\Delta\mathcal{H} = -\frac{1}{2}\sum_{\alpha}\Omega_\alpha b_\alpha^\dagger b_\alpha \hat{x}_\alpha - \frac{\bar{E}_{\rm CC}}{4}(b_1 - b_1^\dagger)(b_2 - b_2^\dagger)\sum_{\alpha}\hat{x}_\alpha. \tag{8}$$

For the transmon at the flux sweet spot it is $\hat{x}_1 = \delta\hat{\phi}_1^2/2$ and for transmon 2 instead $\hat{x}_2 = \tan\phi_2\delta\hat{\phi}_2$, where $\delta\hat{\phi}_\alpha$ are quantized phase fluctuations. $\Delta\mathcal{H}$ conserves the parity of the total number of the two-transmon excitations. Thus it does not connect the states $|\pm\rangle$ to the ground state which, to the first order in V, takes the form $|g\rangle \propto |00\rangle + a_{11}|11\rangle + \sum_{ij=1,2} a_{0j}|0, 2j\rangle + a_{i0}|2i, 0\rangle$. Disregarding thermal excitation processes to higher-energy states, the only effect of flux quantum noise is inside the bi-dimensional subspace $\{|\pm\rangle\}$. By solving a Bloch–Redfield master equation [33], relaxation and decoherence times in the SWAP subspace are given by the usual relation $T_2^{\rm SWAP} = 2T_1^{\rm SWAP} = \{\frac{1}{16}\sum_\alpha(\sin\eta + (-1)^\alpha\cos\eta\bar{E}_{\rm CC}/\Omega_\alpha)^2 S_{x_\alpha}(\omega_{+-})\}^{-1}$ (a pure dephasing term $\propto S_{x_\alpha}(0)$ is disregarded with respect to defocusing due to $1/f$ noise).

The main contribution comes from linear phase fluctuations of the transmon displaced from the sweet spot, $\hat{x}_2$. At low temperatures $k_{\rm B}T \ll \Omega_\alpha$, the flux quantum noise is $S_{x_2}(\omega) \approx (\Omega_2\tan\phi_2)^2(\pi M/\Phi_0)^2 2\omega/R$. For typical parameters we estimate $T_2^{\rm SWAP} \approx 30\,{\rm s}$ at optimal coupling ($M = 140\Phi_0/A$, $R \sim 50\,\Omega$) [13]. Thus the efficiency of the optimized gate on the SWAP time scale is not limited by relaxation processes due to flux noise. This is illustrated in figure 4 where we plot the *envelope* of the concurrence, $C(t)$, which in the presence of $1/f$ noise and flux quantum noise reads

$$C(t) \approx \{[\sin\eta(\rho_{++}(t) - \rho_{--}(t)) + 2\cos\eta\,{\rm Re}\{\rho_{+-}(t)\}]^2 + 4\,{\rm Im}\{\rho_{+-}(t)\}^2\}^{1/2}. \tag{9}$$

Here the population difference in the SWAP subspace is $\rho_{++}(t) - \rho_{--}(t) = (\cos\eta - \delta_{\rm eq}){\rm e}^{-t/T_1^{\rm SWAP}} + \delta_{eq}$, with $\delta_{\rm eq}$ the thermal equilibrium value, and $\rho_{+-}(t) \equiv \langle\rho_{+-}(t)\rangle{\rm e}^{-t/T_2^{\rm SWAP}}$. We observe that for optimal coupling Bell inequality violation, guaranteed until [34] $C(t) \geqslant 2^{-1/2}$, occurs for times $\sim 75\,\mu$s, much longer than for generic coupling.

In the cQED architecture each transmon is dispersively coupled to a resonator used for control and readout. An important mechanism for T_1 processes is spontaneous emission through

the resonator (Purcell effect) [13, 24]. If each transmon operates at positive resonator–transmon detunings, $\Delta_\alpha = \omega_{r\alpha} - \Omega_\alpha \sim 500\,\mathrm{MHz} \gg g_\alpha \sim 50\,\mathrm{MHz}$, where g_α is the transmon–resonator coupling strength, the spontaneous emission rate of the coupled transmons is due to the 'single-mode' Purcell effect [18, 24]. To evaluate it we rewrite $\mathcal{H}$, equation (3), in the basis of its perturbative eigenstates and perform the rotating wave approximation eliminating terms describing the simultaneous excitation (de-excitation) of one resonator and the coupled-transmons system. The restriction to the subspace $\{|g\rangle, |\sigma = \pm\rangle\}$ reads

$$\mathcal{H} + \sum_\alpha \omega_{r\alpha}\, a_\alpha^\dagger a_\alpha + \sum_{\alpha,\sigma=\pm} (g_{\alpha,\sigma}|g\rangle\langle\sigma|a_\alpha^\dagger + \text{h.c.}), \tag{10}$$

where $g_{\alpha,\sigma} = \mathrm{i}\sqrt{2}\beta_\alpha e V_\alpha (E_{J\alpha}/2E_{C\alpha})^{1/4}\langle g|(b_\alpha - b_\alpha^\dagger)|\sigma\rangle$. The eigenstates of (10) are obtained by treating the last term in first-order perturbation theory. The ground state is unmodified and reads $|g, 0_1, 0_2\rangle$, where $|m_\alpha\rangle$ are Fock states of the αth resonator, $m_\alpha \in N$. The corrections to the states $|\sigma, m_1, m_2\rangle$ read $|\sigma, m_1, m_2\rangle^{(1)} = \frac{g_{1\sigma}\sqrt{m_1+1}}{E_\sigma - E_g - \omega_{r1}}|g, m_1+1, m_2\rangle + \frac{g_{2\sigma}\sqrt{m_2+1}}{E_\sigma - E_g - \omega_{r2}}|g, m_1, m_2+1\rangle$, where E_σ and E_g are the unperturbed eigenenergies of (10). The spontaneous decay rate is obtained applying Fermi's golden rule to the interaction Hamiltonian of each resonator with its harmonic bath. The transition rate from the coupled transmons plus resonators state $|\sigma, 0_1, 0_2\rangle + |\sigma, 0_1, 0_2\rangle^{(1)}$ to the ground state $|g, 0_1, 0_2\rangle$ is

$$w_\sigma = 2\sum_\alpha \kappa_\alpha \left|\frac{g_{\alpha,\sigma}}{E_\sigma - E_g - \omega_{r\alpha}}\right|^2, \tag{11}$$

where κ_α is the spontaneous emission rate of the oscillator α and we considered single-photon losses to each bath. The coupled-transmons SWAP levels experience a Purcell-induced spontaneous emission rate reduced with respect to the sum of the resonators spontaneous emission rates. For identical transmons in cavities with a lifetime $1/\kappa_\alpha \approx 160\,\mathrm{ns}$ we estimate $1/w_\sigma \approx 16\,\mu\mathrm{s}$ (analogous to the transmon's relaxation time predicted in [13]), signaling a limitation to the optimized gate efficiency. We expect that the recently proposed Purcell filter or protection schemes [25] can be suitably extended to the considered two-qubit gate which is based on independent readout, possibly overcoming Purcell limitation.

5. Conclusions

In conclusion, we demonstrated the optimization of a cQED *entangling* gate against any relevant $1/f$ noise source while keeping the hardware simplicity of the fixed coupling and even if one qubit does not operate at optimal bias point. The estimated high performance of the gate signals the effective elimination of leading order effects of $1/f$ noise.

Our analysis included all the relevant noise sources acting *during* the entanglement-generating operation in the considered architecture. We have shown that the proposed scheme is robust with respect to relaxation processes due to quantum noise and it is likely to foresee a design protected also from the Purcell effect. Additional errors during readout may of course influence the overall gate fidelity of any specific implementation [9]. The responsible error sources need to be independently eliminated. However, the value of the optimal coupling is not affected by minimization of error sources acting before/after the coupled-qubits evolution. Similarly, for qubit-based quantum information [35], optimization of single- and two-qubit quantum operations is a key requirement, even though the overall quantum processor will suffer from error sources in between quantum operations or at preparation/readout.

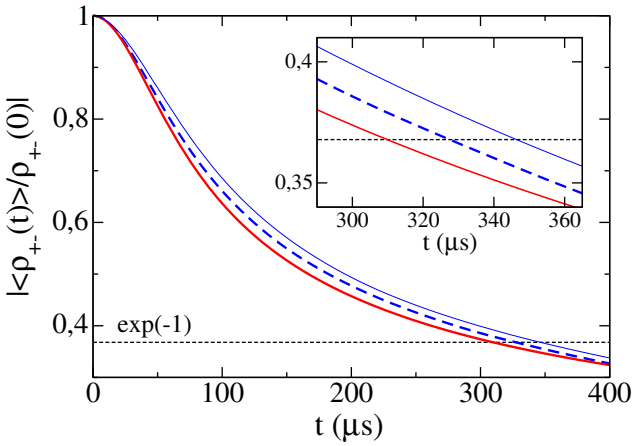

Figure A.1. Absolute value of the coherence $\langle\rho_{+-}(t)\rangle/\rho_{+-}(0)$ in the presence of $1/f$ flux noise on qubit 2 with $\Sigma_{x_2} = 10^{-4}$. The (thick) red line is the result of the SPA, the (thin) blue line is the numerical evaluation of the adiabatic approximation (A.1) for $\gamma_{m2} = 1\,\mathrm{s}^{-1}$, $\gamma_{M2} = 10^6\,\mathrm{s}^{-1}$ as in [31] and the dashed blue line is for $\gamma_{m2} = 1\,\mathrm{s}^{-1}$, $\gamma_{M2} = 10^5\,\mathrm{s}^{-1}$: the smaller the high-frequency cut-off γ_{M2}, the closer the SPA to the adiabatic approximation. Inset: zoom around the time range where $\rho_{+-}(t)/\rho_{+-}(0) \approx \mathrm{e}^{-1}$. Other parameters are $E_{C\alpha} = 1\,\mathrm{GHz}$, $E^0_{J\alpha} = 30\,\mathrm{GHz}$ and $E_{CC} = 1.68 \times 10^7\,\mathrm{Hz}$ ($\bar{E}_{CC} \approx 65\,\mathrm{MHz}$). In the simulations we considered an ensemble of $\sim 10^3$ random telegraph noise processes with switching rates distributed as $\propto 1/\gamma$ in $[\gamma_{m2}, \gamma_{M2}]$. The average is performed using 10^6 realizations of the stochastic process.

Eliminating decoherence remains the biggest challenge for superconducting systems. Further optimization may require, on the one hand, suppression of higher-order effects of $1/f$ noise and, on the other hand, limitation of relaxation due to quantum noise. Concerning intrinsic noise sources, like those responsible for $1/f$ noise, material engineering at the microscopic scale may be required in the near future. 'Passive' optimization strategies may be conveniently combined with 'active' control tools, like dynamical decoupling protocols inspired by nuclear magnetic resonance, which have already been applied to superconducting systems [31, 36]. On a longer time scale, imperfections in the coherent control might represent the ultimate limit to computer performance.

Acknowledgments

We gratefully acknowledge discussions with G Falci and information about ongoing experiments by D Vion. This work was partially supported by the EU through grant no. PITN-GA-2009-234970 and by the Joint Italian–Japanese Laboratory on 'Quantum Technologies: Information, Communication and Computation' of the Italian Ministry of Foreign Affairs.

Appendix. Validity regime of the static path approximation

The SPA is valid for times $t < 1/\gamma_{M\alpha}$. Thus it applies to the considered $\sqrt{\mathrm{i-SWAP}}$ operation if $t_\mathrm{E} = \pi/2\omega_{+-} \approx 10^{-1}$–$10^{-2}\,\mathrm{GHz} < 1/\gamma_{M\alpha}$. Since flux noise is the most relevant $1/f$ noise source

in the considered setup, here we disregard critical current fluctuations and consider the recent noise figures reported in [31]. In that paper, $1/f$ flux noise extends up to ~ 1 MHz; thus we can reasonably expect that the condition $t_{\rm E} < 1/\gamma_{M\alpha}$ is satisfied.

Moreover, we numerically verified that the SPA is a valid approximation also for times $t > 1/\gamma_M$ provided that γ_M is smaller than the system oscillation frequency [29]. In figure A.1, we report the coherence between the states $|\pm\rangle$ in the SPA and the result of the numerical evaluation of the adiabatic approximation

$$\rho_{+-}(t) = \rho_{+-}(0) \int \mathcal{D}[\{x_\alpha(s)\}]\, P[\{x_\alpha(s)\}]\, \mathrm{e}^{-\mathrm{i}\int_0^t \mathrm{d}s\, \omega_{+-}(\{x_\alpha(s)\})}, \tag{A.1}$$

where $\omega_{+-}(\{x_\alpha(s)\}) \approx \sum_\alpha \frac{\partial \omega_{+-}}{\partial x_\alpha} x_\alpha(s) + \frac{1}{2}\sum_{\alpha,\beta} \frac{\partial^2 \omega_{+-}}{\partial x_\alpha \partial x_\beta} x_\alpha(s) x_\beta(s)$ and the derivatives are as reported in section 3 below equation (6). In the figure, we considered flux noise on qubit 2, $x_2(s)$, distributed with $\Sigma_{x_2} = 10^{-4}$ and $\gamma_{m2} = 1\,\mathrm{s}^{-1}$, $\gamma_{M2} = 10^6\,\mathrm{s}^{-1}$ [31]. It is clearly seen that the SPA is a reasonable approximation up to times $\sim 10^2/\gamma_{M2}$. This legitimates the use of the SPA for the evaluation of the times $T_2^{*\mathrm{SWAP}}$ reported in figure 3. The error with respect to an estimate based on the adiabatic approximation is $\sim 10\%$ (inset of figure A.1).

References

[1] Clarke J and Wilhelm F K 2008 *Nature* **453** 1031

[2] Nakamura Y *et al* 1999 *Nature* **398** 786
Yu *et al* 2002 *Science* **296** 889
Martinis J M *et al* 2002 *Phys. Rev. Lett.* **89** 117901
Chiorescu I *et al* 2003 *Science* **299** 1869
Yamamoto T *et al* 2003 *Nature* **425** 941
Saito S *et al* 2004 *Phys. Rev. Lett.* **93** 037001
Johansson J *et al* 2006 *Phys. Rev. Lett.* **96** 127006
Deppe F *et al* 2008 *Nature Phys.* **4** 686

[3] Vion D *et al* 2002 *Science* **296** 886

[4] Pashkin Yu A *et al* 2003 *Nature* **421** 823
Berkley A J *et al* 2003 *Science* **300** 1548
Yamamoto T *et al* 2003 *Nature* **425** 941
Majer J B *et al* 2005 *Phys. Rev. Lett.* **94** 090501
Plantenberg J H *et al* 2007 *Nature* **447** 836
Izmalkov A *et al* 2004 *Phys. Rev. Lett.* **93** 037003
Hime T *et al* 2006 *Science* **314** 1427
Niskanen A O *et al* 2007 *Science* **316** 723
Majer J *et al* 2007 *Nature* **449** 443
van der Ploeg S H W *et al* 2007 *Phys. Rev. Lett.* **98** 057004
Fay A *et al* 2008 *Phys. Rev. Lett.* **100** 187003

[5] McDermott R *et al* 2005 *Science* **307** 1299
Steffen M *et al* 2006 *Science* **313** 1423

[6] Ansmann M *et al* 2009 *Nature* **461** 504
Palacios-Laloy A *et al* 2010 *Nature Phys.* **6** 442

[7] Blais A *et al* 2004 *Phys. Rev* A **69** 062320

[8] Majer J *et al* 2007 *Nature* **449** 443
Sillanpää M A *et al* 2007 *Nature* **449** 438
Bialczak R C *et al* 2010 *Nature Phys.* **6** 409

[9] Dewes A *et al* 2012 *Phys. Rev. Lett.* **108** 057002
[10] DiCarlo L *et al* 2010 *Nature* **467** 574
[11] Dewes A *et al* 2012 *Phys. Rev.* B **85** 140503(R)
[12] DiCarlo L *et al* 2009 *Nature* **460** 240
[13] Koch J *et al* 2007 *Phys. Rev.* A **76** 042319
[14] Schreier J A *et al* 2008 *Phys. Rev.* B **77** 180502
[15] Wellstood F C *et al* 1987 *Appl. Phys. Lett.* **50** 772
Van Harlingen D J *et al* 2004 *Phys. Rev.* B **70** 064517
[16] Preskill J 1998 *Proc. R. Soc. Lond.* A **454** 385
[17] Paik H *et al* 2011 *Phys. Rev. Lett.* **107** 240501
[18] Mallet F *et al* 2009 *Nature Phys.* **5** 791
[19] Gywat O *et al* 2006 *Phys. Rev.* B **73** 125336
[20] Rebić S *et al* 2009 *Phys. Rev. Lett.* **103** 150503
[21] Paladino E *et al* 2010 *Phys. Rev.* B **81** 052502
[22] Paladino E *et al* 2011 *New J. Phys.* **13** 093037
[23] Verstaete F and Wolf M 2002 *Phys. Rev. Lett.* **89** 170401
[24] Houck A A *et al* 2008 *Phys. Rev. Lett.* **101** 080502
[25] Reed M D *et al* 2010 *Appl. Phys. Lett.* **96** 203110
Gambetta J M *et al* 2011 *Phys. Rev. Lett.* **106** 030502
[26] Chow J M *et al* 2011 *Phys. Rev. Lett.* **107** 080502
[27] Catelani G *et al* 2011 arXiv:1106.0829
[28] Koch J *et al* 2009 *Phys. Rev. Lett.* **103** 217004
[29] Falci G *et al* 2005 *Phys. Rev. Lett.* **94** 167002
[30] Ithier G *et al* 2005 *Phys. Rev.* B **72** 134519
[31] Bylander J *et al* 2011 *Nature Phys.* **7** 565
[32] Wooters W K 1998 *Phys. Rev. Lett.* **80** 2245
Yu T and Eberly J H 2006 *Phys. Rev. Lett.* **97** 140403
[33] Cohen-Tannoudji C, Dupont Roc J and Grynberg G 1998 *Atom–Photon Interactions* (New York: Wiley-Interscience)
[34] Verstraete F and Wolf M M 2002 *Phys. Rev. Lett.* **89** 170401
[35] Nielsen M and Chuang I 2005 *Quantum Computation and Quantum Information* (Cambridge: Cambridge University Press)
[36] Falci G *et al* 2004 *Phys. Rev.* A **70** 040101